CONTRIBUTION TO SESSION A1E

CERN-PRE-78-186

ANIZATION FOR NUCLEAR RESEARCH

PARTICLE AND ANTIPARTICLE PRODUCTION BY 200 AND 210 GeV PROTONS IN THE CERN - SPS CHARGED HYPERON BEAM

M. Bourquin [2], R.M. Brown [5], Y. Chatelus [6], J.C. Chollet [4], M. Croissiaux [6], A. Degré [6], D. Froidevaux [4], A.R. Fyfe [1], C.N.P. Gee [5], J-M. Gaillard [4], M. Gibson [1], P. Igo-Kemenes [3], P. W. Jeffreys [1], B. Merkel [4], R. Morand [6], H. Plothow [*], J-P. Repellin [4], G. Sauvage [4], B.J. Saunders [5], B. Schiby [6], H. W. Siebert [3], V. J. Smith [1], K. P. Streit [3], R. Strub [6], J. J. Thresher, J. Trischuk [5]

Bristol [1], Geneva [2], Heidelberg [3], Orsay [4], RHEL [5], Strasbourg [6]
Collaboration

A B S T R A C T

We have measured the production of $\pi^+, K^+, p, \Sigma^+, \overline{\Sigma^-}, \overline{\Xi^-}, d$ and $\pi^-, K^-, \bar{p}, \Sigma^-, \overline{\Sigma^+}, \Xi^-, \Omega^-, \bar{d}$ in the forward direction for $0.35 \leq x \leq 0.65$. This range of x corresponds to laboratory momenta between 70 and 130 GeV/c for an incident proton momentum of 200 GeV/c. Particles are identified by a DISC Cerenkov counter, and decay products are analyzed by a magnetic spectrometer. Antihyperon $(\overline{\Sigma^-}, \overline{\Xi^-}, \overline{\Sigma^+})$ and Ω^- fluxes have been measured for the first time in a hyperon beam.

In the comparison of our data with results from other experiments, we observe scaling behaviour and $(1-x)^n$ distribution for inclusive particle production.

1) H.H. Wills Physics Laboratory, University of Bristol, Bristol, England.

2) Université de Genève, Suisse.

3) Physikalisches Institut, Universität Heidelberg, Philosophenweg 12, D-69 Heidelberg, B.R.D.

4) Laboratoire de l'Accélérateur linéaire, Université Paris Sud, bâtiment 200, F-91405 Orsay, France.

5) Rutherford Laboratory, Chilton, Didcot OX11 OQX, England.

6) C.R.N. Division des hautes Energies, F-67037 Strasbourg Cedex, France.

*) CERN Fellow, 1211 Genève 23, Suisse.

I. INTRODUCTION

We present the results of the measurement of particle and anti-particle fluxes in the CERN SPS charged hyperon beam. This beam uses a DISC Cerenkov counter to identify secondary particles produced in the forward direction from interactions of 200 and 210 GeV/c protons. In order to study the decays of the hyperons in the beam, a magnetic spectrometer is used to measure the charged final state particles.

II. HYPERON BEAM

Protons extracted from the SPS interact in a 32 cm long BeO target placed inside the first bending magnet M1 (Fig. 1). This magnet separates the secondary particles from the transmitted protons, which are absorbed in the first collimator C_1. Magnets M2 and M3, which are filled with a dense material except for a narrow channel of 3 cm^2 in cross section on average, further reduce the background and select a beam whose central momentum can be varied up to 130 GeV/c. In order to match the acceptance of the DISC, the beam is focused to be parallel, using the superconducting quadrupoles Q_1 and Q_2. Under typical running conditions, the momentum bite of the secondary particles at the end of the magnetic channel is ±8%.

The momentum dispersion of the beam and the optical properties of the magnetic channel allow the particle momenta to be determined from their horizontal angles. This is done with five multiwire proportional chambers (Fig. 2), using staggered planes to give an effective wire spacing of 0.25 mm. The accuracy is ±1% on the momentum and ±0.07 mrad on the angles in projection.

III. THE DISC CERENKOV COUNTERS

The SPS DISC is of the type described by Ref. 1). The Cerenkov angle (40 mrad) and the radiator length (2m) have been chosen to minimize the decay losses; the gas (CO_2) and the correcting optics to optimize Ξ and Σ separation at 150 GeV/c. Eight photomultiplier tubes collect the light transmitted through a circular diaphragm whose width can be varied to change the acceptance. The pressure can be varied to cover the range of velocities corresponding to masses up to 5 GeV/c^2 if the beam is set at 100 GeV/c. Pressure curves are shown in Figs. 3 and 4 for negative and positive beams at 100 GeV/c. For part of the experiment a second and shorter DISC, used in a previous PS experiment [2], has been installed to extend the mass range up to 10 GeV/c^2.

IV. THE SPECTROMETER

Drift chambers before and after the spectrometer magnet (Fig.2) are used to measure the charged particles from hyperon decays. The magnet has an integrated strength of 2.2 T.m. . The main parameters of the two drift chamber telescopes are the following :

(a) in front of the magnet : drift space 5 mm, spatial accuracy 200 μ which corresponds to a 0.1 mrad angular accuracy;

(b) after the magnet : drift space 10 mm, spatial accuracy 300 μ which corresponds also to a 0.1 mrad angular accuracy.

The resulting momentum resolution of the system is ±1.5% at 100 GeV/c. The relative calibration of the spectrometer and the magnetic channel has been achieved using beam pions traversing all the apparatus. The accuracy of the spectrometer using $\Xi^- \rightarrow \Lambda\pi^-$ decays is shown on Figs. 5 and 6. The FWHM of the reconstructed Λ and Ξ^- masses are 4 MeV/c^2 and 6 MeV/c^2, respectively. Additional detectors are used to identify electrons and photons and to measure their energies.

V. PARTICLE FLUXES AND RATIOS

The fluxes of the most abundant particles $(\pi^\pm, K^\pm, p, \bar{p}, \Sigma^\pm, \Xi^-)$ at the exit of the DISC are determined from the pressure curves (Figs. 3 and 4 for 100 GeV/c). For the less abundant particles $(\bar{\Sigma}^\pm, \bar{\Xi}^-, \Omega^-, d, \bar{d})$ which do not appear as a peak in pressure curves because of the low signal to background ratio, information from the spectrometer is used. The reconstruction efficiency has been measured using the abundant decay $\Xi^- \rightarrow \Lambda\pi^-$, $\Lambda \rightarrow p\pi^-$. In the case of $\overline{\Sigma^{\mp}}$ one also requires a reconstructed π^0 from the $\overline{\Sigma^+} \rightarrow \bar{p}\pi^0$ decay; the efficiency of reconstructing a π^0 is known from the $\Sigma^+ \rightarrow p\pi^0$ events. The fluxes are corrected for the geometrical acceptance of the DISC and Table 1 gives the fluxes obtained at the 98.5 GeV/c for 10^6 outgoing particles. At present we have reconstructed 12 $\overline{\Sigma^+}$, 204 $\overline{\Xi^-}$ and ~ 1700 Ω's. The particle ratios at the production target are determined from the fluxes at the DISC taking into account the decay losses in the magnetic channel and the absorption in the production target. These ratios are given in Table 2 for 70, 95, 100, 120, 130 GeV/c . The systematic error of ±15% has been estimated from the reproducibility of the measurements and is mainly due to different beam conditions.

In Figs. 7 and 8 particle ratios K^+/π^+, K^-/π^-, $\bar{p}/\pi^-$ and p/π^+ are plotted as function of the Feynman variable x and compared to other existing data at other energies [3]. One notices a good agreement between our data and the high energy data; the scaling behaviour of production seems to appear at energies above 100 GeV.

Figures 9 and 10 show the Σ^-/π^-, Σ^+/π^+ and Ξ^-/π^- particle ratios as functions of x compared to low energy data [4]. Our 210 GeV data are in agreement with the 24 GeV PS data, but in disagreement with the 29.7 GeV AGS data. As the low energy data disagree one cannot draw a conclusion about the scaling behaviour of hyperon production.

The production of particles in the forward direction at large x is generally described by an invariant cross section $Ed^3\sigma/d^3p \sim$ $\sim (1-x)^n$, where n depends upon the particle. Assuming this type of dependence, the values $\Delta n = (n_i - n_\pi)$ are shown in Figs. 7 to 10 for the ratios of the various particles to pions. For the baryons p, Σ^- and Ξ^- the power n_i increases with strangeness making the leading particle effect less and less pronounced.

In Fig. 11 the particle ratios p/π, Σ/π, Ξ/π, Ω/π and the antiparticle to particle ratios $\bar{p}/p$, $\overline{\Sigma^+}/\Sigma^+$, $\overline{\Xi^-}/\Xi^-$ are plotted as functions of the strangeness. One observes the rapid decrease of the leading particle production (p,Σ,Ξ,Ω) and the rapid rise of the antiparticle to particle ratio with the baryon strangeness.

VI. HIGH MASS SEARCH

Using both DISCs we have searched for high mass particles produced by 200 GeV protons at a momentum of 95 GeV/c. Data have been taken for a range of mass between 2 and 10 GeV/c^2 by varying the pressures of the 2 DISC counters and for negative and positive polarities. The steps in pressure have been chosen to ensure a complete coverage of the mass range by the mass acceptances of the DISCs. An additional gas Cerenkov counter has been used to eliminate random particles which triggered one DISC. This counter, installed just after the two DISCs has a Cerenkov threshold set at a mass of 2 GeV/c^2 for a momentum of 95 GeV/c.

In the analysis, we have looked first for "stable" particles, i.e., particles not decaying before the end of the apparatus. This corresponds to particles of lifetime greater than $m \times 10^{-9}$ sec where m is the mass in GeV/c^2. Having found no particle, we can set a limit for the production ratio X^+/π^+ or X^-/π^- of $X/\pi \leq 10^{-7}$ with 90% confidence, for $x = 0.475$. This corresponds to a cross section of 7 nb/GeV/c/sr per nucleus using measured pion cross sections [5]. This experiment extends similar attempts at observing high mass metastable particles [5)-6)] with smaller lifetimes by a factor of 10 to 100. We have looked also for particle decays by searching for events with kinks between tracks measured at the DISC and the spectrometer. The main background is due to off-momentum stable particles with the right momentum to trigger the DISC and interacting in the decay region. This background is eliminated by requiring that the momentum p measured by the spectrometer is not equal to $(m/m_o)p_o$ where m_o is the DISC mass setting, m the mass of π, K or p and p_o the nominal momentum. Having found no event after this cut, we can also set a limit on the particle ratio at the DISC, which is $X/\pi \leq 10^{-7}$ with 90% confidence. Due to the shorter decay length the limit applies to particles with a lifetime smaller by a factor 3.

VII. CONCLUSIONS

With the CERN SPS charged hyperon beam we have measured charged particle ratios for both signs and for a large number of particles at various momenta between 70 and 130 GeV/c. In particular we have measured hyperon fluxes Σ^-, Ξ^-, Ω^- high enough to allow a study of the leptonic decays of Σ^- and Ξ^- and to collect a sample of about 2000 Ω's [7].

Antihyperons $(\overline{\Sigma^+}, \overline{\Xi^-})$ have been isolated for the first time in a charged hyperon beam.

REFERENCES

1) C. Bovet et al., The CEDAR Project, CERN LabII/EA/74-4 (Rev. August 1975).

2) J. Badier et al., Phys.Letters 39B, 414 (1972).

3) J. Singh et al., CHLM collaboration - to be published in Nuclear Physics B;

W.F. Baker et al., Phys.Letters 51B, 303 (1974);

FSAS : D.S. Ayres et al., Phys.Rev. D15, 3105 (1977);

Yu.B. Bushin et al., Phys.Letters 29B, 48 (1963);

J.V. Allaby et al., CERN report No. 70-12 (1970) - unpublished;

U. Amaldi et al., Nuclear Phys. B86, 403 (1975).

4) J. Badier et al., Phys.Letters 39B, 414 (1972);

V. Hungerbühler et al., Phys.Rev. D12, 1203 (1975).

5) J.A. Appel et al., Phys.Rev.Letters 32, 428 (1974).

6) W. Bozzoli et al., submitted to Nuclear Physics B.

7) Measurement of the lifetime and branching ratios of the Ω^-, paper submitted to this conference.

FIGURE CAPTIONS

1. Hyperon beam.
2. Spectrometer layout.
3. Pressure curve at 100 GeV for negative particles.
4. Pressure curve at 100 GeV for positive particles.
5. Reconstructed Λ mass.
6. Reconstructed Ξ^- mass.
7. K^+/π^+, K^-/π^-, $\bar{p}/\pi^+$ ratios as functions of x.
8. p/π^+ ratio as function of x.
9. Σ^+/π^+, Σ^-/π^- ratios as functions of x.
10. Ξ^-/π^- ratio as function of x.
11. p/π, Σ/π, Ξ/π, Ω/π and $\bar{p}/p$, $\bar{\Sigma}/\Sigma$, $\overline{\Xi^-}/\Xi^-$ ratios as functions of S.

*****

TABLE CAPTIONS

1. Fluxes at 100 GeV for positive and negative particles at the DISC.
2. Particle ratios at production target for 70, 95, 100, 120, 130 GeV/c.

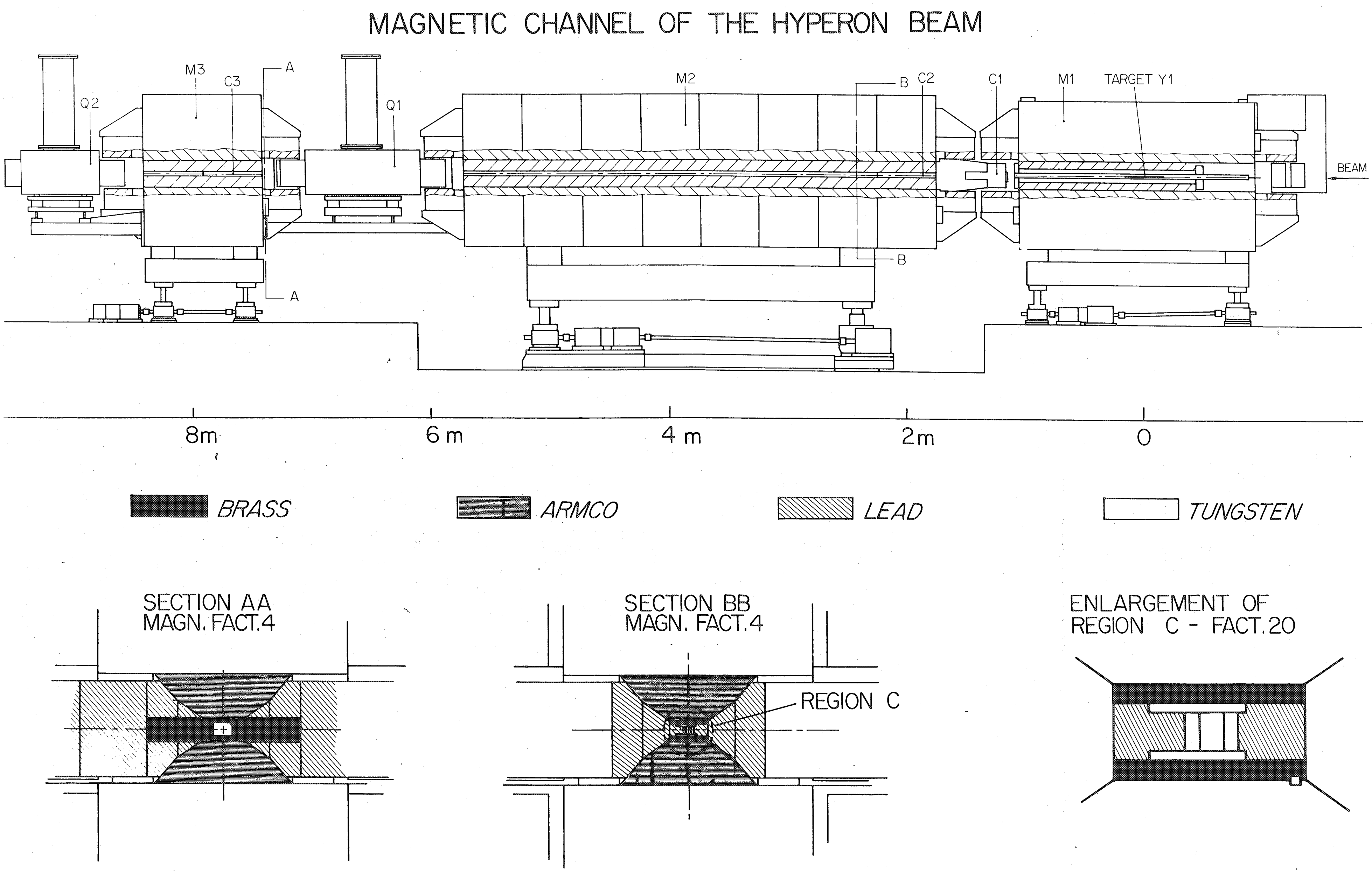
MAGNETIC CHANNEL OF THE HYPERON BEAM
Q2
M3
C3
A
Q1
M2
B
C2
C1
M1
TARGET Y1
BEAM
8m
6 m
4 m
2m
0
BRASS
ARMCO
LEAD
TUNGSTEN
SECTION AA
MAGN. FACT.4
SECTION BB
MAGN. FACT.4
REGION C
ENLARGEMENT OF
REGION C - FACT.20

Fig.1

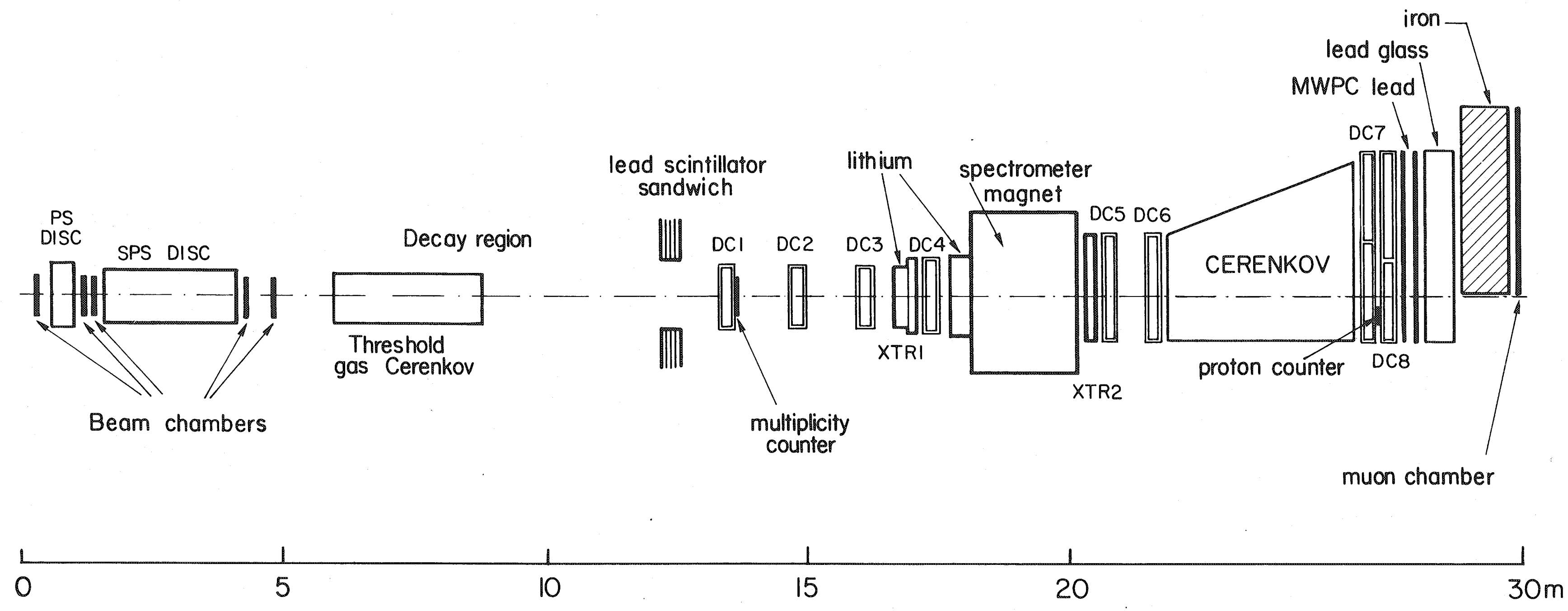
PS
DISC
SPS DISC
Beam chambers
Decay region
Threshold
gas Cerenkov
lead scintillator
sandwich
DC1
DC2
DC3
DC4
multiplicity
counter
lithium
XTR1
spectrometer
magnet
XTR2
DC5 DC6
CERENKOV
proton counter
DC7
DC8
MWPC lead
lead glass
iron
muon chamber
0
5
10
15
20
30m

Fig.2

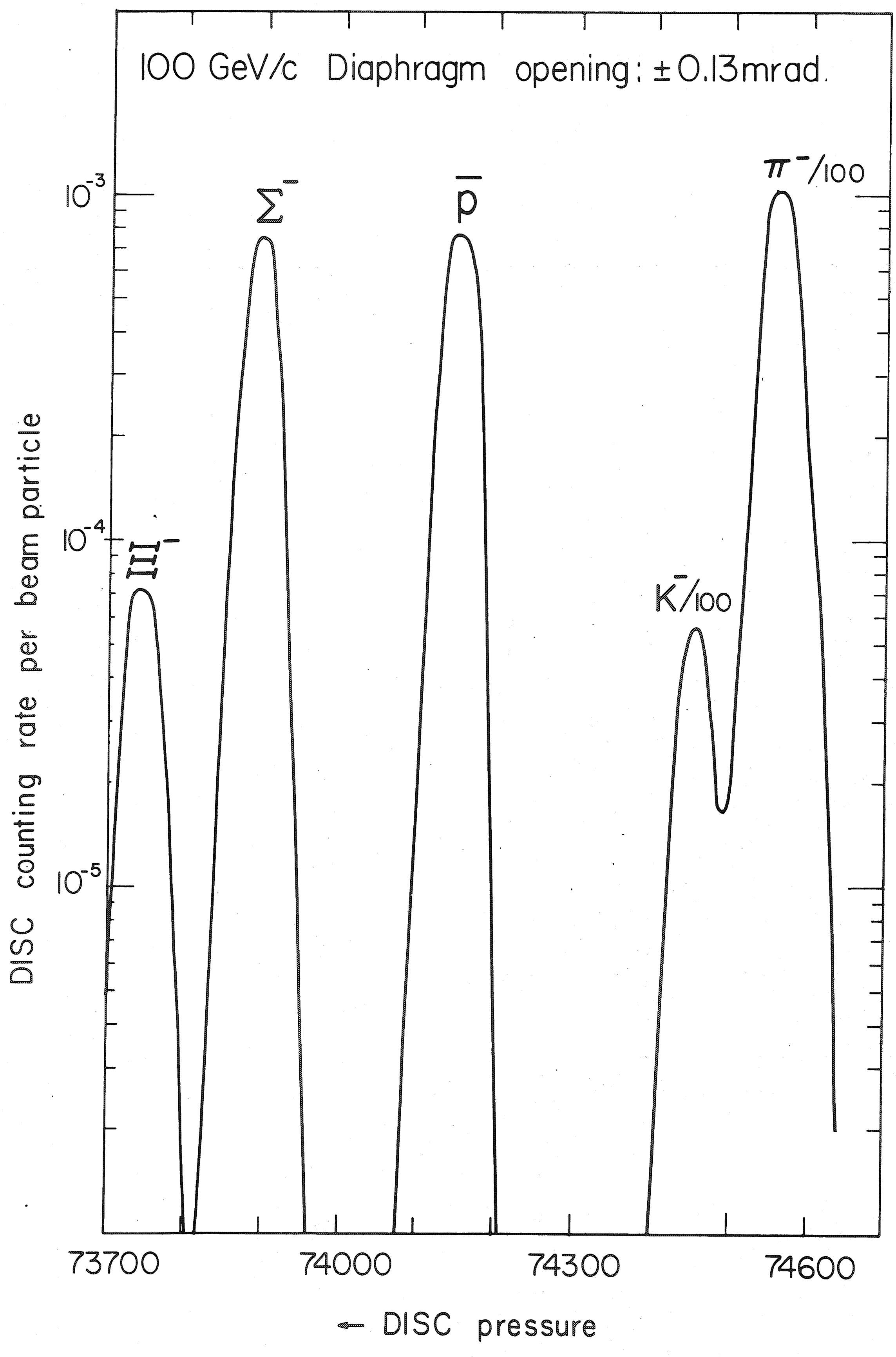
100 GeV/c Diaphragm opening: ±0.13mrad.
10^{-3}
10^{-4}
10^{-5}
Ξ^-
Σ^-
$\bar{p}$
$K^-/100$
$\pi^-/100$
DISC counting rate per beam particle
73700
74000
74300
74600
← DISC pressure

Fig.3

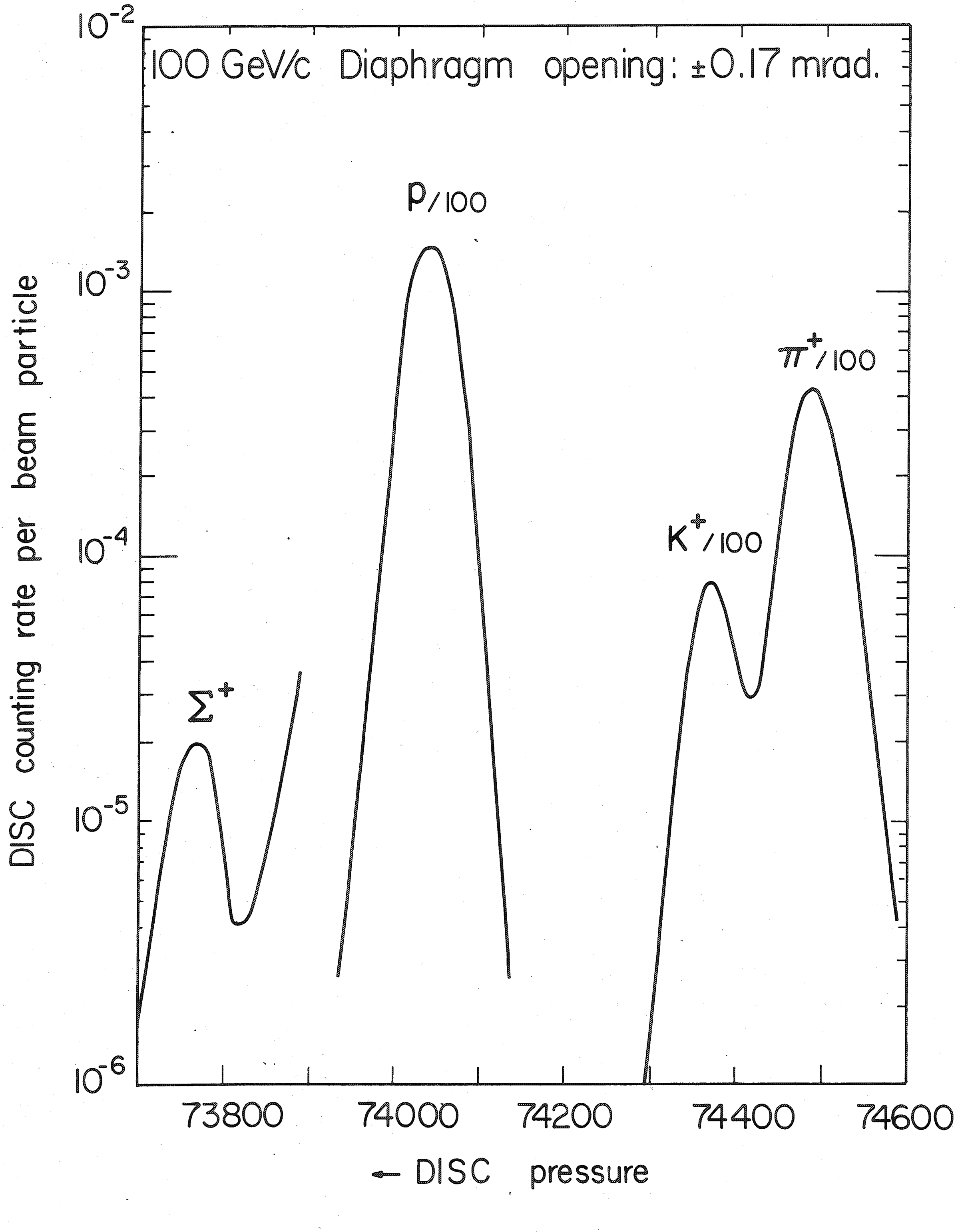

100 GeV/c Diaphragm opening: ±0.17 mrad.
p/100
Σ^+
K^+/100
π^+/100
DISC counting rate per beam particle
10^{-2}
10^{-3}
10^{-4}
10^{-5}
10^{-6}
73800
74000
74200
74400
74600
← DISC pressure

Fig.4

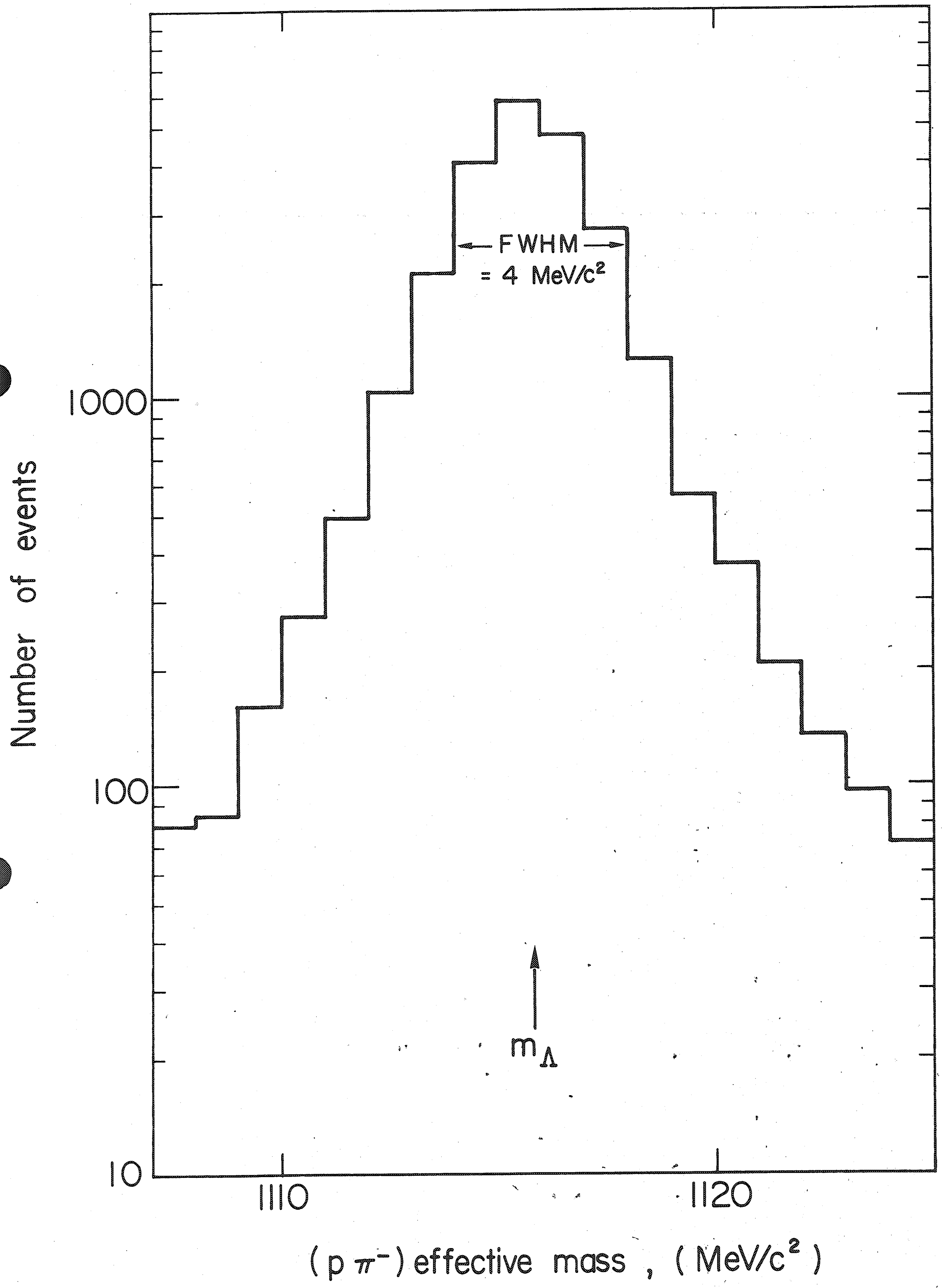

FWHM
= 4 MeV/c²
1000
100
10
Number of events
m_Λ
1110
1120
(p π^-) effective mass , (MeV/c²)

Fig.5

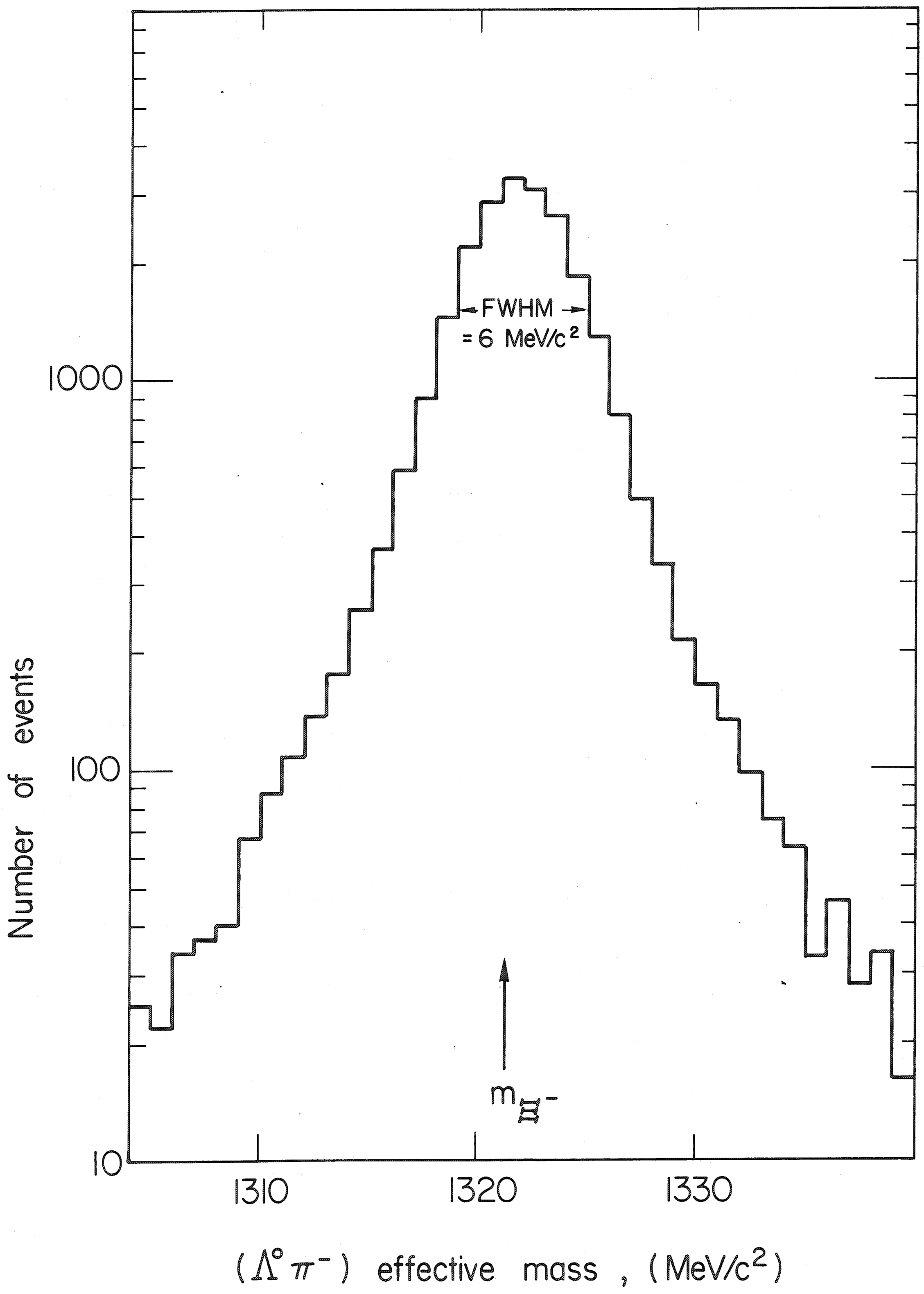

Number of events
1000
100
10
FWHM
= 6 MeV/c²
m_{Ξ^-}
1310
1320
1330
$(\Lambda^{\circ}\pi^{-})$ effective mass , (MeV/c²)

Fig.6

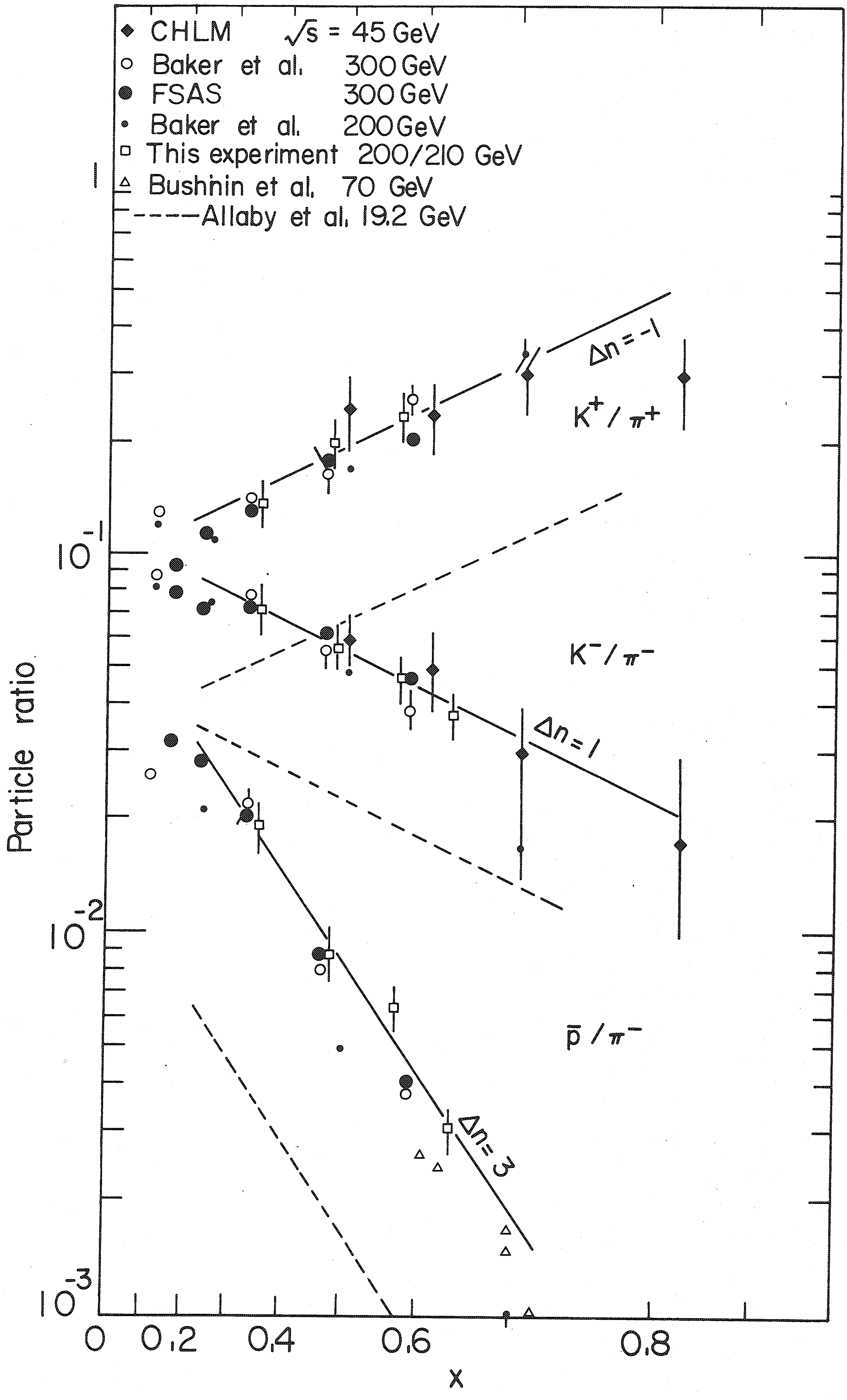
◆ CHLM √s = 45 GeV
○ Baker et al. 300 GeV
● FSAS 300 GeV
• Baker et al. 200 GeV
□ This experiment 200/210 GeV
△ Bushnin et al. 70 GeV
----Allaby et al. 19.2 GeV
Δn=-1
K+ / π+
K- / π-
Δn=1
p̄ / π-
Δn= 3
Particle ratio
1
10-1
10-2
10-3
0
0.2
0.4
0.6
0.8
x

Fig.7

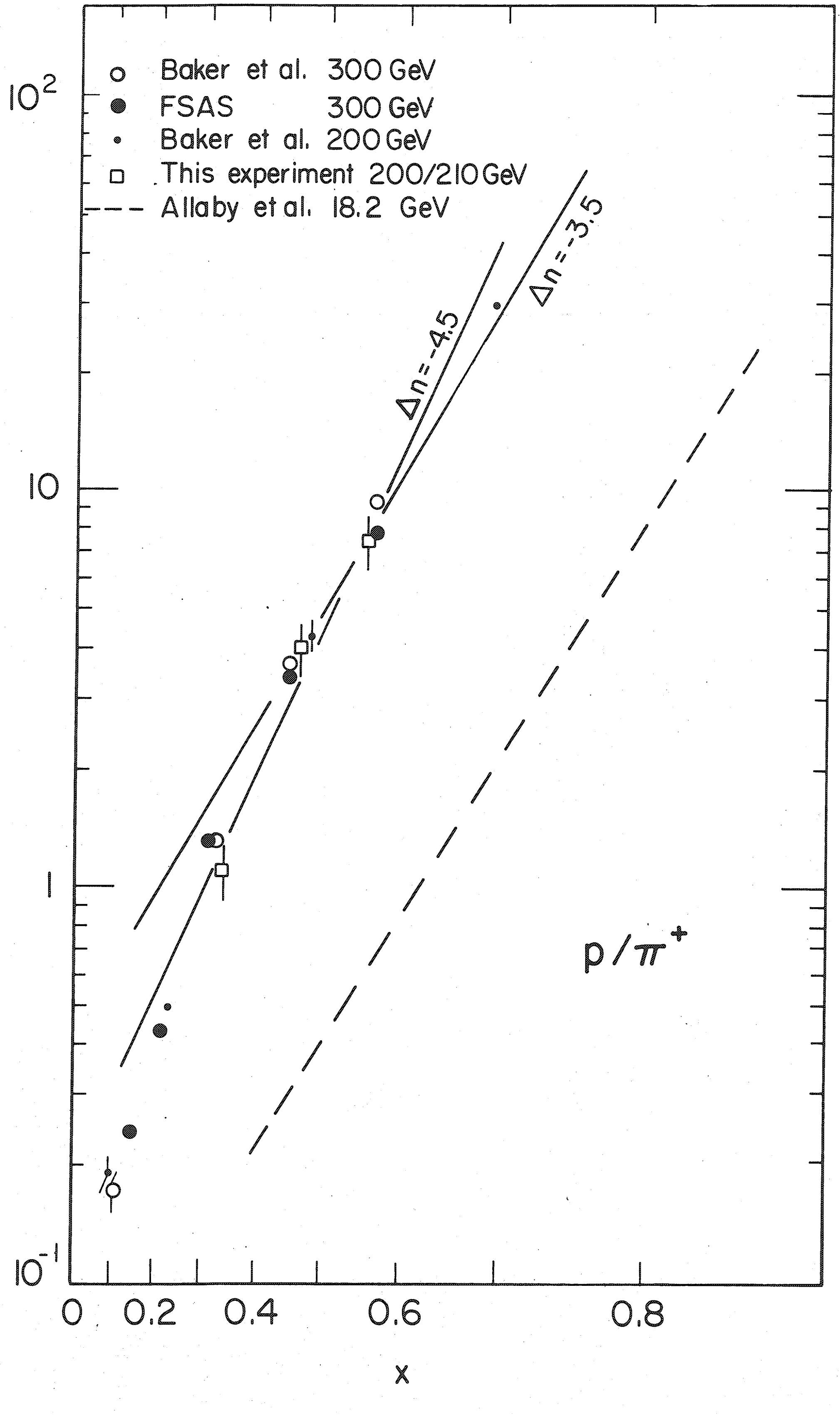

Baker et al. 300 GeV
FSAS 300 GeV
Baker et al. 200 GeV
This experiment 200/210 GeV
Allaby et al. 18.2 GeV
$\Delta n = -4.5$
$\Delta n = -3.5$
p/π^+
10^2
10
1
10^{-1}
0
0.2
0.4
0.6
0.8
x

Fig.8

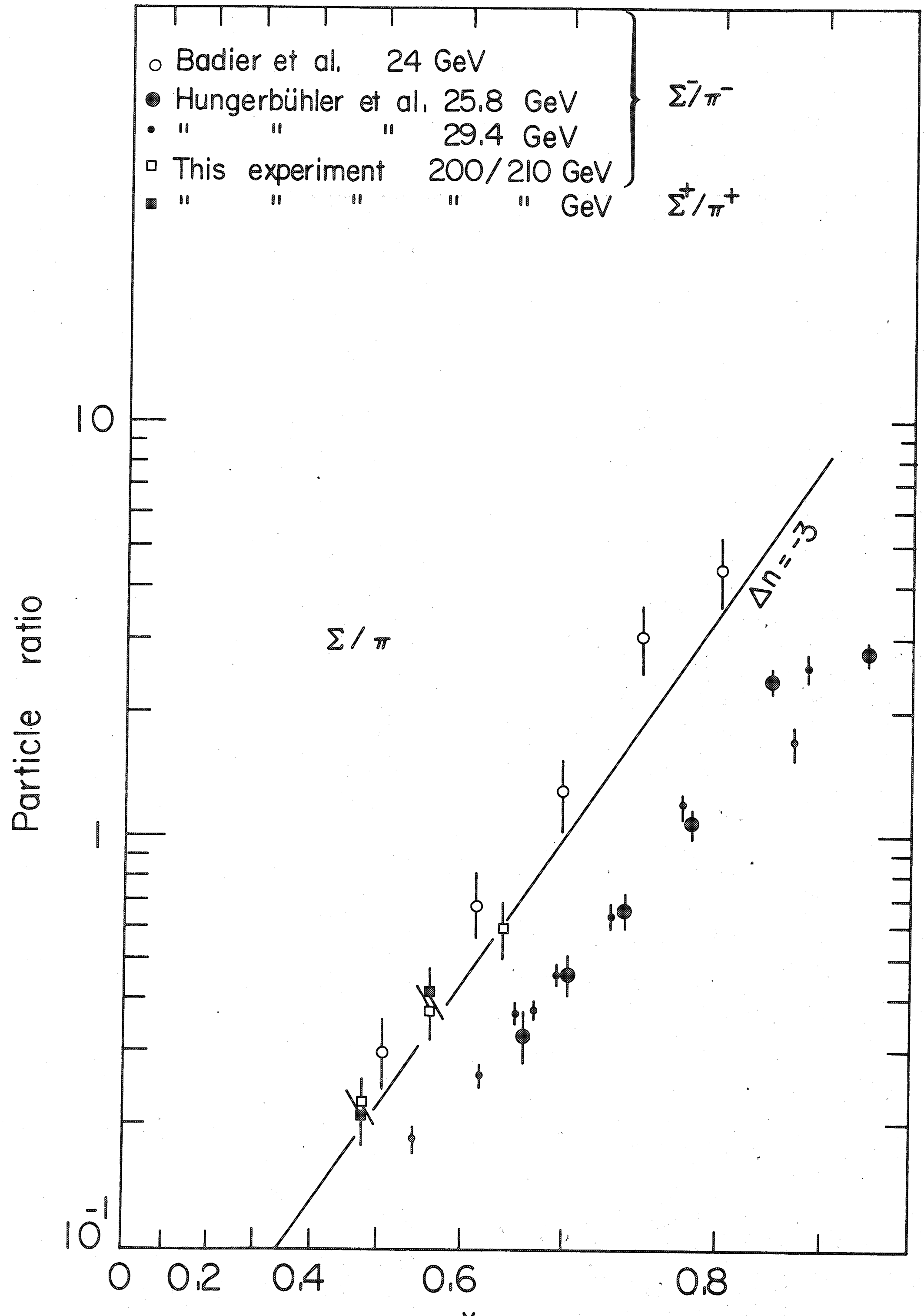

○ Badier et al. 24 GeV
● Hungerbühler et al. 25.8 GeV
• " " " 29.4 GeV
□ This experiment 200/210 GeV
■ " " " " " GeV
Σ^-/π^-
Σ^+/π^+
Particle ratio
Σ/π
$\Delta n = -3$
10
1
10^{-1}
0
0.2
0.4
0.6
0.8
x

Fig.9

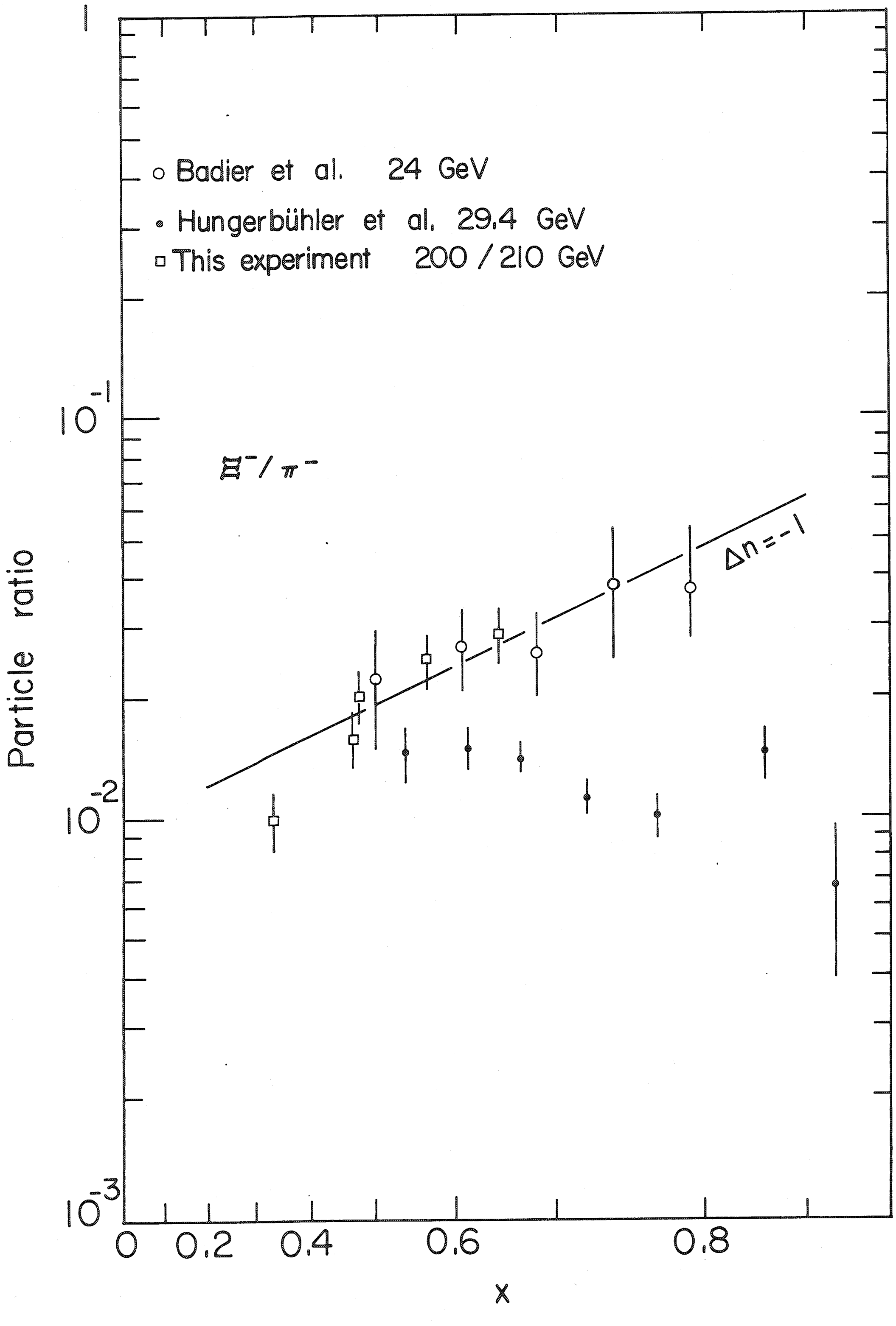
o Badier et al. 24 GeV
• Hungerbühler et al. 29.4 GeV
□ This experiment 200 / 210 GeV
Ξ⁻/π⁻
Δn = -1
Particle ratio
1
10⁻¹
10⁻²
10⁻³
0
0.2
0.4
0.6
0.8
X

Fig.10

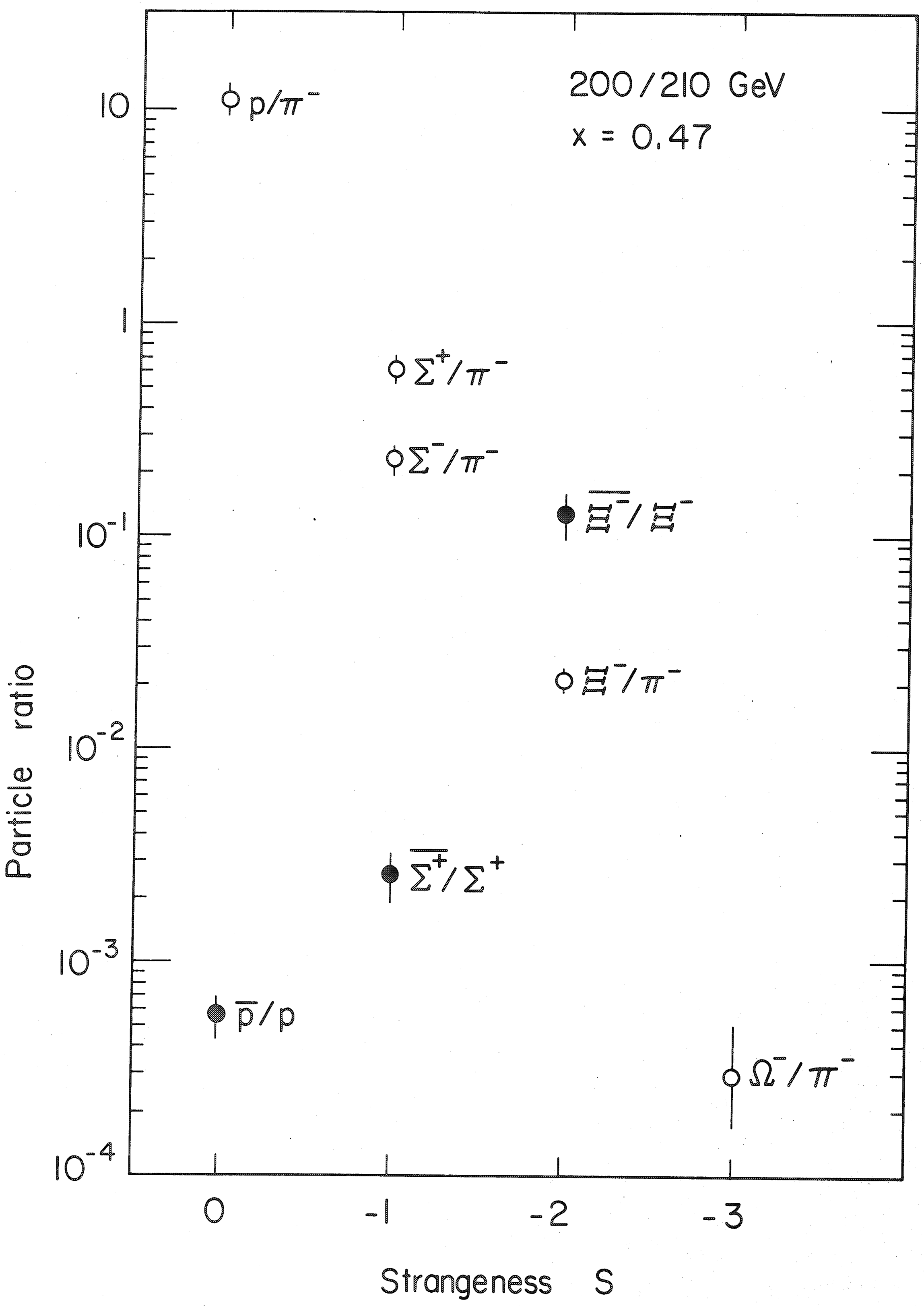
200/210 GeV
x = 0.47
p/π⁻
Σ⁺/π⁻
Σ⁻/π⁻
Ξ̄⁻/Ξ⁻
Ξ⁻/π⁻
Σ̄⁺/Σ⁺
p̄/p
Ω⁻/π⁻
10
1
10⁻¹
10⁻²
10⁻³
10⁻⁴
Particle ratio
0
-1
-2
-3
Strangeness S

Fig.11

Table 1

Hyperon fluxes signed by the DISC under typical running conditions at 98.5 GeV/c.

	Σ^-	$\overline{\Sigma^+}$	Ξ^-	Ω^-	Σ^+	$\overline{\Xi^-}$
Fluxes	4000	2	400	0.1	50	2

These numbers correspond to 10^6 secondary particles coming out from the magnetic channel. They have been obtained by using, for each particle, a specially optimised diaphragm, in order to maximise the DISC acceptance, and, at the same time,ensure a sufficient rejection against particles of neighbouring mass.

Table II

Particle ratios at production

	200 GeV/c protons		210 GeV/c protons		
	95 GeV/c	128 GeV/c	73 GeV/c	98.5 GeV/c	115 GeV/c
K^-/π^-	$(4.8\pm0.7)10^{-2}$	$(3.8\pm0.6)10^{-2}$	$(7.2\pm1.1)10^{-2}$	$(5.6\pm0.8)10^{-2}$	$(4.7\pm0.7)10^{-2}$
$\bar{p}/\pi^-$	$(7.9\pm1.2)10^{-3}$	$(3.1\pm0.46)10^{-3}$	$(1.9\pm0.3)10^{-2}$	$(8.9\pm1.3)10^{-3}$	$(6.4\pm0.9)10^{-3}$
Σ^-/π^-	0.195 ± 0.029	0.60 ± 0.009	$(8.0\pm1.2)10^{-2}$	0.229 ± 0.034	0.380 ± 0.057
$\overline{\Sigma^+}/\pi^-$	$(1.5\pm0.4)10^{-3}$				
Ξ^-/π^-	$(1.62\pm0.24)10^{-2}$	$(2.9\pm0.43)10^{-2}$	$(1.0\pm0.15)10^{-2}$	$(2.1\pm0.3)10^{-2}$	$(2.5\pm0.4)10^{-2}$
Ω^-/π^-				$(2.9\pm0.4)10^{-4}$ x $e^{\pm0.56}$	
$\bar{d}/\pi^-$	$(2.5\pm1.7)10^{-7}$ (2events seen)				
K^+/π^+			0.14 ± 0.02	0.20 ± 0.03	0.235 ± 0.035
p/π^+			1.11 ± 0.22	3.95 ± 0.59	7.5 ± 1.1
Σ^+/π^+				0.21 ± 0.03	0.42 ± 0.06
$\overline{\Xi^-}/\pi^+$				$(1.3\pm0.2)10^{-3}$	
d/π^+	$(2.4\pm0.5)10^{-4}$				